Supplement of Atmos. Meas. Tech., 18, 5841–5859, 2025 https://doi.org/10.5194/amt-18-5841-2025-supplement © Author(s) 2025. CC BY 4.0 License.





### Supplement of

# A new technique to retrieve aerosol vertical profiles using micropulse lidar and ground-based aerosol measurements

Bo Chen et al.

Correspondence to: Sarah D. Brooks (sbrooks@tamu.edu)

The copyright of individual parts of the supplement might differ from the article licence.

#### S1. Processing Normalized Relative Backscatter from raw signal

MPL and MiniMPL receive a raw signal that is described as:

$$raw(R) = \frac{O_c(R)ECR^{-2}\beta(R)T(R)^2 + n_b + n_{ap}(R)}{D[raw(R)]}$$
(S1)

5

R is the range of the lidar;  $O_c$  is the overlap contribution, which describes the compromised optical efficiency of the lidar at the near field due to the incomplete geometric overlap of the receiver field of view and the beam width;  $n_b$  represents the background contribution;  $n_{ap}$  represents the afterpulse contribution caused by the saturation of the detector diode due to internal scattering at the start of each scan; D[raw(R)] is the "dead time" factor which is unique for each detector and is a function of the raw signal; E is the lidar laser energy output; E0 is the system calibration constant; E1 is the backscatter coefficient; E2 is the transmittance (Campbell et al., 2002). After applying corrections for the overlap, afterpulse, "dead time" factor, and the background signal, the classic lidar equation can be obtained:

15

$$P(R) = \frac{\{raw(R) \times D[raw(R)]\} - n_{ap}(R) - n_b}{O_c(R)} = ECR^{-2}\beta(R)T(R)^2$$
 (S2)

The range and energy normalized relative backscatter (also known as attenuated backscatter) is calculated as:

$$NRB(R) = \frac{P(R) \cdot R^2}{E} = C\beta(R)T(R)^2$$
 (S3)

20

By expanding Equation SI. 3 for a 2-component atmosphere, we get

$$NRB(R) = C[\beta_1(R) + \beta_2(R)]T_1^2(R)T_2^2(R)$$
 (S4)

#### **S2. Overlap Correction Function**

25

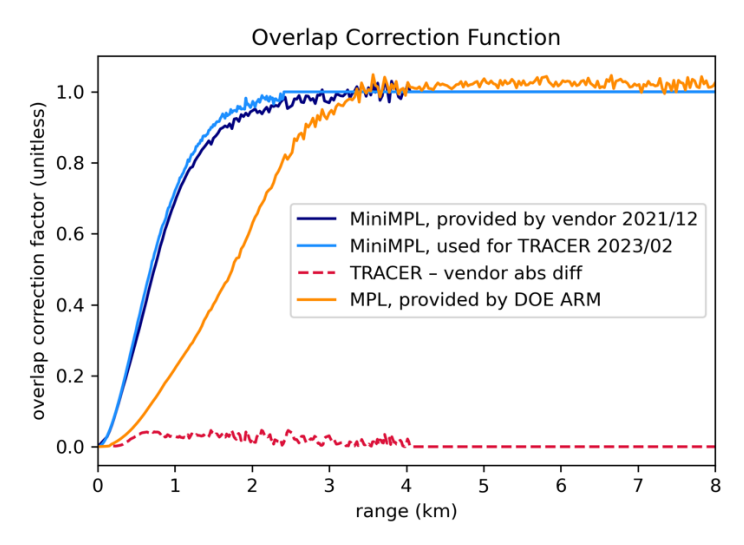


Figure S1 TAMU MiniMPL overlap function used for TRACER is shown in a solid light blue line, and the overlap function provided by the vendor is shown in a solid dark blue line. The difference between the overlap function used for TRACER and the overlap function provided by DOE ARM is shown in a dashed red line. ARM supplied the MPL overlap function shown in the orange line.

"Overlap" refers to the near-range mismatch between the outgoing laser beam and the detector's field of view, which prevents full signal capture. Droplet Measurement Technologies provided a default overlap function (Dec 2021) and a method for recalibration (Welton and Campbell, 2002). Following their method, we recalibrated the miniMPL overlap on February 21, 2023, by aligning the instrument horizontally to collect calibration data. As shown in Figure R1, the vendor and post-campaign overlap functions are similar. However, small differences of up to 10.9% were observed at close range (~0.5 km), which decrease to <5% by 1 km. We used the post-campaign overlap due to its closer timing to TRACER. The ARM MPL overlap function was supplied by the ARM program.

#### S3. Numerical calculations of the Fernald inversion

0 The numerical form of Equation 2 for the backwards retrieval from a calibration range at far field is:

$$A(I, I+1) = (S_1 - S_2)[\beta_2(I) + \beta_2(I+1)]\Delta R$$

$$\beta_1(I-1) + \beta_2(I-1) = \frac{NRB(I-1) \cdot exp[+A(I-1,I)]}{\frac{NRB(I)}{\beta_1(I) + \beta_2(I)} + S_1 \{NRB(I) + NRB(I-1) \cdot exp[+A(I-1,I)]\}\Delta R}$$
(S5)

Therefore, the total backscatter coefficient of each layer can be calculated with the total backscatter coefficient of the layer above. The total backscatter coefficient profile can thus be calculated iteratively once the total backscatter coefficient at the calibration range is given. The  $\Delta R$  matches the vertical resolution of lidar data and is 15 meters for ARM MPL and 30 meters for MiniMPL. A new calibration constant  $\frac{NRB(I)}{\beta_1(I)+\beta_2(I)}$  at step *I*-1 is calculated using the backscatter coefficient at step *I* (Gimmestad and Roberts, 2023).

#### 50 S4. Sensitivity of NRB Profiles to Time-Averaging Window

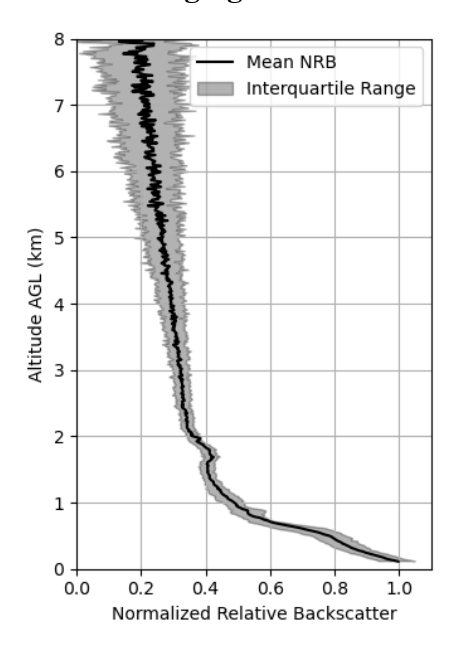


Figure S2 Mean (solid black line) and interquartile range (gray area) of NRB profiles for the example case on 28 August 2022.

We assess the uncertainty associated with temporal variability of attenuated backscatter by calculating the interquartile range (25th–75th percentile) of the 1-minute NRB profiles within the averaging window.

For the example case (in the Method section) on 28 August shown in the figure above, the relative magnitude of temporal variability in NRB is comparable to the retrieval uncertainty presented in Figure 4b of the main manuscript. Because range-dependent noise grows with height, the temporal average of NRB shows greater variability aloft; the backscatter coefficient profile retrieval steps apply smoothing to reduce this noise, so the retrieved backscatter profile has lower uncertainty at those heights.

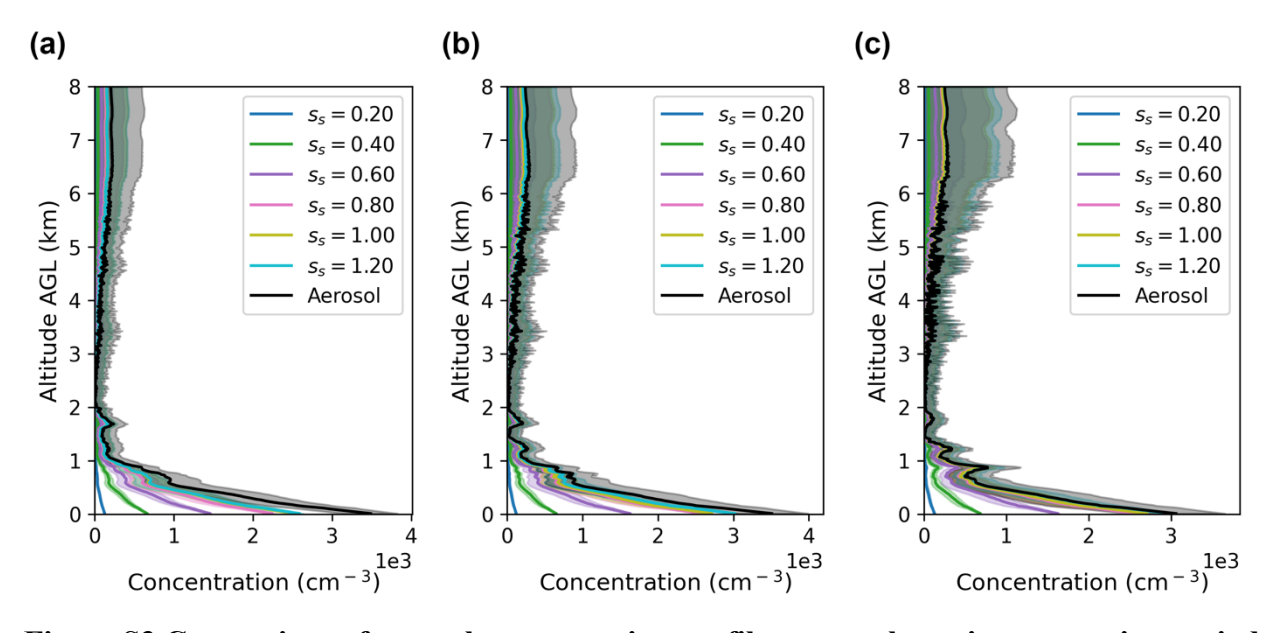
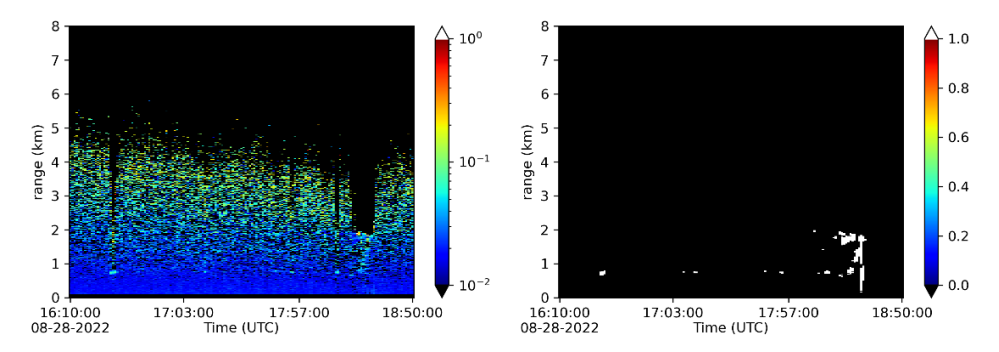


Figure S3 Comparison of aerosol concentration profile among three time-averaging periods for the example case on 28 August 2022 (a) 2 hr 40 min averaging time (b) 1 hr averaging time (c) 30 minute averaging.

To demonstrate the sensitivity of our retrieval method to the time averaging window, we compare the aerosol and CCN concentration profile collected on 28 August using three averaging windows—2 hr 40 min, 1 hr, and 30 min—each centered on the 17:28 UTC radiosonde launch. The three averaging windows comprise 131, 55, and 29 individual lidar profiles, respectively. The overall shape and magnitude of aerosol concentration profiles remain largely consistent across all three averaging windows. However, small differences still appear, reflecting short-term variability in the aerosol field. The 30-minute average (Figure 1c) is also noticeably noisier and has more uncertainties at higher altitudes.

#### S5. Depolarization Ratio and Cloud Masking

80



## Figure S4 Depolarization ratio and cloud mask time series for 28 August 2022, with MiniMPL in Galveston, Texas

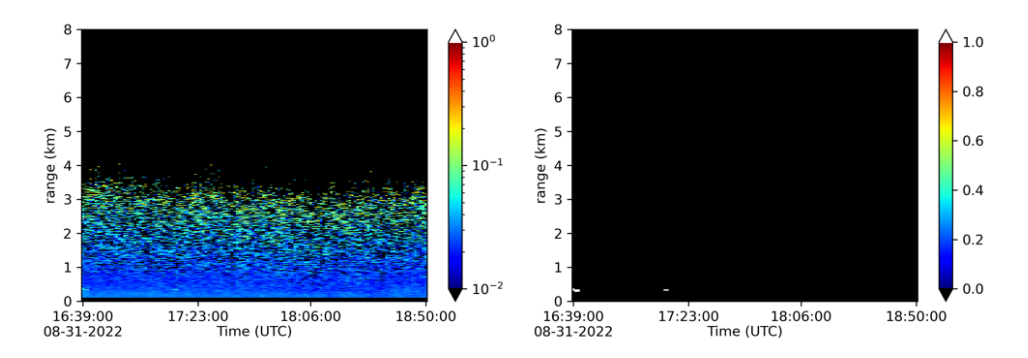


Figure S5 Depolarization ratio and cloud mask time series for 31 August 2022, with MiniMPL in Galveston, Texas

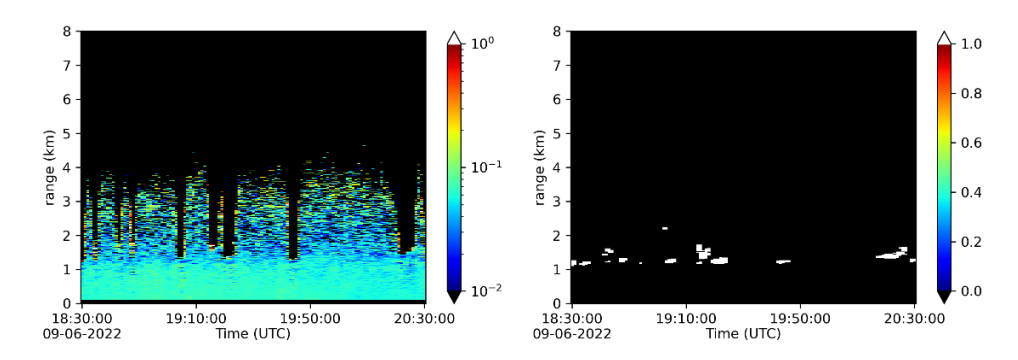
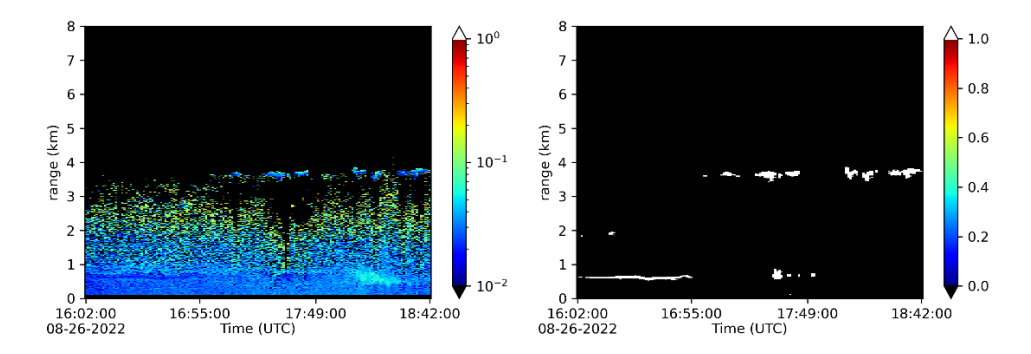


Figure S6 Depolarization ratio and cloud mask time series for 6 September 2022, with MiniMPL in Hockley, Texas



5 Figure S7 Depolarization ratio and cloud mask time series for 26 August 2022, with MiniMPL in Galveston, Texas

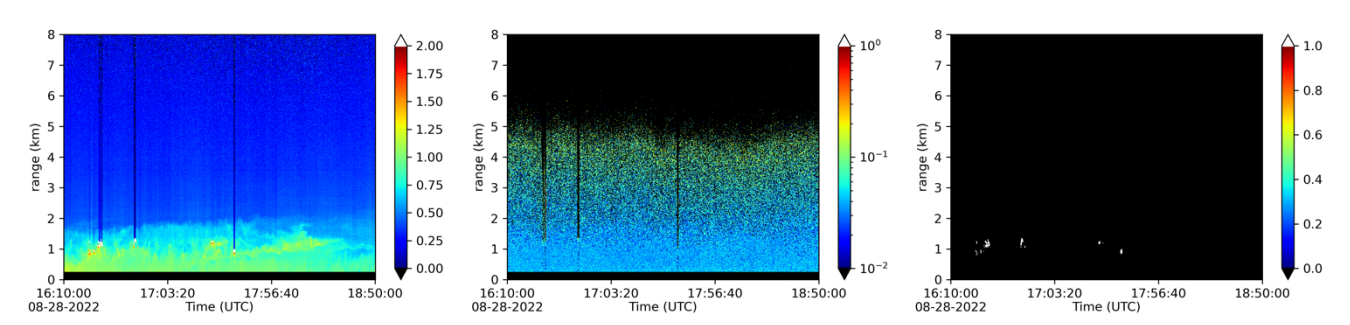


Figure S8 NRB, depolarization ratio, and cloud mask time series for 28 August 2022, with ARM AMF-1 MPL in LaPorte, Texas

#### **S6. References**

100

Campbell, J. R., Hlavka, D. L., Welton, E. J., Flynn, C. J., Turner, D. D., Spinhirne, J. D., Scott III, V. S., and Hwang, I.: Full-time, eye-safe cloud and aerosol lidar observation at atmospheric radiation measurement program sites: Instruments and data processing, Journal of Atmospheric and Oceanic Technology, 19, 431-442, <a href="https://doi.org/10.1175/1520-0426(2002)019%3C0431:ftesca%3E2.0.co;2">https://doi.org/10.1175/1520-0426(2002)019%3C0431:ftesca%3E2.0.co;2</a>, 2002.

Gimmestad, G. G. and Roberts, D. W.: Lidar engineering: introduction to basic principles, Cambridge University Press, https://doi.org/10.1017/9781139014106, 2023.